

## Crystallization and preliminary X-ray analysis of human placental *S*-adenosylhomocysteine hydrolase

MARY A. TURNER,<sup>a</sup> KIRAN DOLE,<sup>a</sup> CHONG-SHENG YUAN,<sup>b</sup> MICHAEL S. HERSHFIELD,<sup>c</sup> RONALD T. BORCHARDT,<sup>b</sup> AND P. LYNNE HOWELL<sup>a,d</sup> at <sup>a</sup>Division of Biochemistry Research, Research Institute, Hospital for Sick Children, Hospital for Sick Children, Toronto, M5G 1X8, Ontario, Canada, <sup>b</sup>Departments of Biochemistry and Pharmaceutical Chemistry, University of Kansas, Lawrence, Kansas 66045, USA, <sup>c</sup>Department of Medicine and Biochemistry, Duke University Medical Center, Durham, North Carolina, 77071, USA, and <sup>d</sup>Department of Biochemistry, Faculty of Medicine, University of Toronto. Medical Sciences Building, Toronto, M5S 1A8, Ontario, Canada. E-mail: howell@aragorn.psf.sickkids.on.ca

(Received 20 September 1996; accepted 26 November 1996)

### Abstract

A recombinant form of human placental *S*-adenosylhomocysteine (AdoHcy) hydrolase expressed in *E. coli*, which was inactivated by a type-I mechanism-based inhibitor, has been crystallized using the hanging-drop vapour-diffusion technique. The crystals grow as flat plates, with unit-cell dimensions  $a = 96.2$ ,  $b = 173.6$ ,  $c = 142.9$  Å,  $\alpha = \beta = \gamma = 90^\circ$ . The crystals exhibit the symmetry of space group *C222* and diffract to a minimum spacing of  $\approx 2.0$  Å resolution at the Cornell High Energy Synchrotron Source. On the basis of density calculations two monomers of the tetrameric protein are estimated to be present in the asymmetric unit ( $V_m = 2.99$  Å<sup>3</sup> Da<sup>-1</sup>). The self-rotation function clearly indicates the location of the non-crystallographic twofold axis.

### 1. Abbreviations

AdoHcy hydrolase, *S*-adenosylhomocysteine hydrolase; AdoHcy, *S*-adenosylhomocysteine; Hcy, homocysteine; Ado, adenosine; AdoMet, *S*-adenosylmethionine; DHCaA, (1'*R*,2'*S*,3'*R*)-9-(2',3'-dihydroxycyclopentan-1'-yl) adenine.

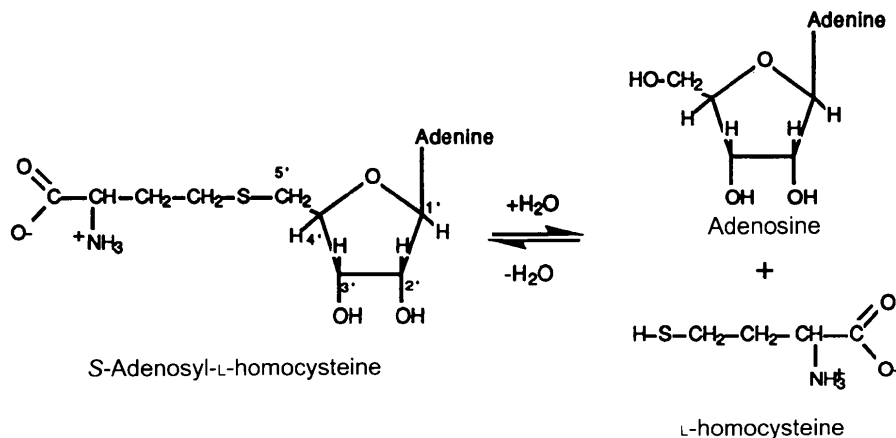
### 2. Introduction

The enzymatic transfer of a methyl group from *S*-adenosylmethionine (AdoMet) to an acceptor molecule, *i.e.* biological transmethylation, is a reaction involved in regulating a diverse array of physiologically important processes. The activities of all AdoMet-dependent methyltransferases are regulated by the

intracellular level of *S*-adenosylhomocysteine (AdoHcy), a product inhibitor of AdoMet-dependent transmethylation (Borchardt, 1980). In all eukaryotic cells, the intracellular level of AdoHcy is regulated by the enzyme AdoHcy hydrolase (Eloranta & Kajander, 1984; Eloranta, Kajander & Raina, 1982) (E.C. 3.3.1.1) which catalyzes the reversible hydrolysis of AdoHcy to adenosine (Ado) and homocysteine (Hcy) (de la Haba & Cantoni, 1959). AdoHcy hydrolase is a highly conserved enzyme, with the human protein sharing  $\sim 70\%$  amino-acid sequence identity with the enzymes from *Dictyostelium* and *Leishmania*, two species that are separated from humans by over a billion years of evolution (Coulter-Karis & Hershfield, 1989; Henderson *et al.*, 1992; Kasir, Aksamit, Backlund & Cantoni, 1988).

AdoHcy hydrolase is a homotetramer of  $\sim 48$  kDa subunits (Fujioka & Takata, 1981; Hershfield, Aiyar, Premakumar & Small, 1985; Palmer & Abeles, 1979; Richards, Chiang & Cantoni, 1978; Ueland, 1982) with one NAD<sup>+</sup> cofactor bound per subunit (Palmer & Abeles, 1976).

Palmer & Abeles (1976, 1979) have elucidated the mechanism by which AdoHcy hydrolase catalyzes the reversible hydrolysis. In the hydrolytic direction, the first step involves the oxidation of the 3' hydroxyl group of AdoHcy by the enzyme bound NAD<sup>+</sup>. This oxidation is followed by the elimination of Hcy to give 3'-keto-4',5'-dehydroadenosine. The Michael addition of water at the 5' position of this tightly bound intermediate to form 3'-ketoadenosine is followed by an NADH-dependent reduction to form Ado. AdoHcy hydrolase was identified as a high-affinity cytoplasmic adenosine-binding protein and the binding of 2'-deoxyadenosine and adenosine



arabinoxidase shown to cause its suicide-like inactivation due to reduction of the enzyme-bound NAD<sup>+</sup> (Abeles, Fish & Lapinskas, 1982; Hershfield, 1979; Hershfield & Kredich, 1978; Hershfield, Small, Premakumar, Bagnara & Fetter, 1982). Inhibition/inactivation of AdoHcy hydrolase has been implicated in causing immunodeficiency in humans, fetal hepatotoxicity in mice, and with deficiency of adenosine deaminase (Hershfield, 1979; Hershfield & Kredich, 1978; Hershfield, Kredich, Ownby, Ownby & Buckley, 1979; Kredich & Martin, 1977; Migchielsen *et al.*, 1995). Deletion of the murine AdoHcy hydrolase gene is also associated with early embryonic death (Miller *et al.*, 1994).

Knowledge of the mechanism of the enzyme has been used extensively in the design of potent and selective inhibitors of AdoHcy hydrolase despite the lack of any detailed information about the tertiary structure and the dynamics of the enzyme. Indeed, inhibitors of this enzyme have already been shown to exhibit antiviral (Liu, Wolfe & Borchardt, 1992; Wolfe & Borchardt, 1991), antiparasitic (Bitoni, Baumann, Jarvi, McCarthy & McCann, 1990; Henderson *et al.*, 1992) anti-arthritis (Wolos, Frondorf & Esser, 1993) and immunosuppressive properties (Wolos, Frondorf, Babcock, Stripp & Bowlin, 1993; Wolos *et al.*, 1993). The therapeutic effects of these inhibitors can, in most cases, be related to their ability to cause an intracellular accumulation of AdoHcy which results in the inhibition of the crucial AdoMet-dependent methylation reactions (Henderson *et al.*, 1992; Liu *et al.*, 1992; Wolfe & Borchardt, 1991). The crystallization and preliminary X-ray analysis of recombinant human placental AdoHcy hydrolase presented in this paper are the first essential steps towards the three-dimensional structure determination of this protein and a clearer understanding of the mechanism of action of this key regulatory enzyme.

### 3. Crystallization and data collection

Earlier attempts to crystallize this enzyme have been unsuccessful and probably failed because conventional purification of the protein leads to heterogeneity in the sample with both the NAD<sup>+</sup> (approximately 90%) and NADH (approximately 10%) forms of the enzyme present. Therefore, the recombinant human placental enzyme, which was purified from cell-free extracts of *E. coli* transformed with the plasmid pPROKcd20 (Coulter-Karis & Hershfield, 1989, 1990), was used to prepare the pure apoenzyme according to previously described procedures (Yuan, Yeh, Liu & Borchardt, 1993). This apoenzyme was then incubated with NAD<sup>+</sup> to yield the pure NAD<sup>+</sup> form of the enzyme (Yuan *et al.*, 1993). The NAD<sup>+</sup> form of the AdoHcy hydrolase was then inactivated with (1'*R*,2'*S*,3'*R*)-9-(2',3'-dihydroxycyclopentan-1'-yl) adenine (DHCaA), a type-I mechanism-based inhibitor (Paisley, Hasobe & Borchardt, 1989; Wolfe & Borchardt, 1991), forming the DHCaA-inactivated enzyme containing one equivalent of NADH and one equivalent of 3'-ketoDHCaA bound to each subunit of the protein.

Initial screening for crystallization conditions was performed using a sparse-matrix screen (Jancarik & Kim, 1991) at room temperature (293 K). All crystals were grown using the hanging-drop vapour-diffusion technique. 5 µl of protein solution (40–60 mg ml<sup>-1</sup>) were added to 5 µl of precipitating solution [12%(w/v) PEG 4K, 20%(v/v) isopropanol, 200 mM ammonium acetate, 100 mM citrate buffer, pH 5.6] on a

Table 1. Diffraction data statistics

No. of measured reflections	269482
No. of independent reflections	56769
No. of crystals	1
Resolution (Å)*	2.22
$R_{\text{merge}}^{\dagger}$	6.8 (14.1)‡
Completeness (%)	85.7 (71.2)‡
Average $I/\sigma(I)$	15.6

\* Resolution limit is defined as the limit beyond which fewer than 50% of the reflections have  $I > 3\sigma(I)$ . Diffraction was observed to at least 2.0 Å resolution. † Defined as  $R = \sum |I(k) - \langle I \rangle| / \sum I(k)$ , where  $I(k)$  and  $\langle I \rangle$  represent the diffraction intensity values of the individual measurements and the corresponding mean values. The summation is over all measurements. ‡ Values given in parentheses refer to reflections in the outer resolution shell, 2.29–2.22 Å.

siliconized glass coverslip and suspended over a 1 ml reservoir containing the same precipitating solution. Some precipitation of the protein occurs immediately and is followed by crystal growth, with flat plate-like crystals appearing in approximately 10–14 d. The crystals grow to a maximal size of 0.8 × 0.5 × 0.1 mm (Fig. 1). Attempts to eliminate the precipitation of the protein prior to crystal growth by varying the protein and precipitant concentrations failed to yield crystals.

Initially, the crystals were mounted in a quartz capillary and data were collected at room temperature on a Siemens Xentronics area detector system with a Rigaku RU-200 rotating anode. The crystals, however, diffracted weakly to a minimum  $d$  spacing of approximately 3.5 Å and suffered significantly from radiation damage. Conditions for freezing the crystals to liquid nitrogen temperatures were, therefore, developed. The crystal was first transferred to a cryoprotectant solution containing 10%(v/v) glycerol, 12%(w/v) PEG 4K, 20%(v/v) isopropanol, 200 mM ammonium acetate, 100 mM citrate buffer, pH 5.6 for approximately 30 min. A rayon CryoLoop (Hampton Research) was used to pick up the crystal which was immediately transferred into a stream of liquid nitrogen maintained at 100 K. The frozen crystals diffracted on the RU-200 X-ray generator to a minimum  $d$  spacing of ~3.1 Å. A complete set of native data has subsequently been collected at Station A1 at the Cornell

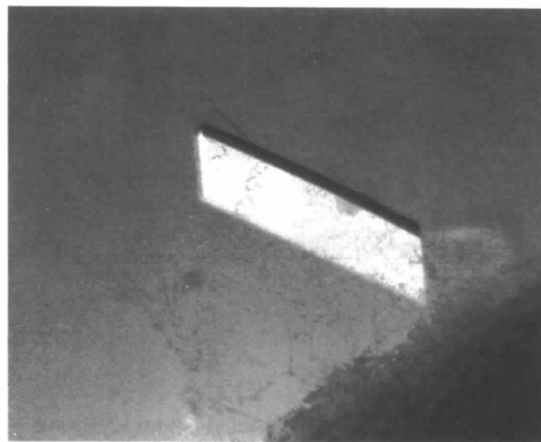


Fig. 1. Crystal of human AdoHcy hydrolase. The crystal is approximately 0.8 × 0.25 × 0.1 mm.

High Energy Synchrotron Source to  $\sim 2.2 \text{ \AA}$  resolution. The data were collected on the ADSC CCD detector with the detector set at two different offset heights to measure the low- and high-resolution data. The data were processed using the program *DENZO* (Otwinowski, 1993). A total of 378  $\varphi$ -scanning oscillation exposures in steps of  $1.5^\circ$  were recorded. A summary of the data-collection statistics is presented in Table 1. The unit-cell dimensions were found to be  $a = 96.2$ ,  $b = 173.6$ ,  $c = 142.9 \text{ \AA}$ ,  $\alpha = \beta = \gamma = 90.0^\circ$ . The crystals display the symmetry of the space group *C222*. On the basis of density calculations, we estimate that two monomers (Matthews parameter  $V_m = 2.99 \text{ \AA}^3 \text{ Da}^{-1}$ ) will be present in the asymmetric unit (Matthews, 1968).

A self-rotation function study has been performed using data between 10 and 6  $\text{\AA}$  resolution to determine the location of the non-crystallographic twofold that relates each monomer in the asymmetric unit. Fig. 2 is the self-rotation function for the  $\kappa = 180^\circ$  section. The unique twofold axis is marked with an arrow and lies  $23^\circ$  from the  $a$  axis. All other peaks on the circumference are identical and are related by the crystallographic twofold axes. The peak is 33.3% of the origin peak, which represents one of the crystallographic twofold axes. The result of this self-rotation study indicate that the tetrameric protein has 222 symmetry, with one of the twofold axes parallel to the crystallographic  $c$  axis, the second twofold is  $23^\circ$  from the  $a$  axis and the third, generated as a consequence of the first two, is  $23^\circ$  from the  $b$  axis. A search for heavy-atom derivatives is currently in progress.

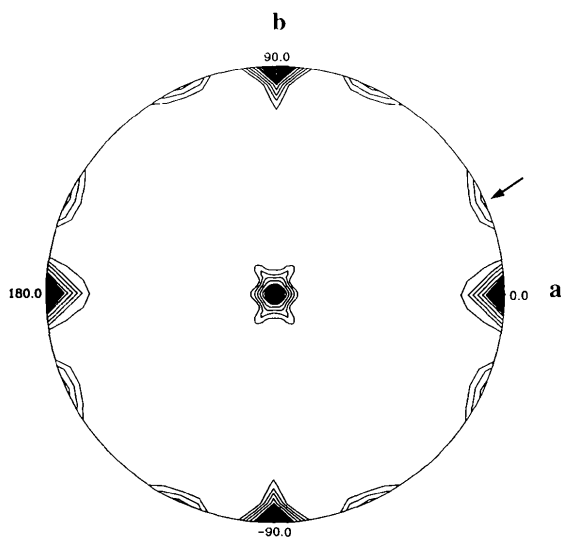


Fig. 2. Self-rotation function showing the  $\kappa = 180^\circ$  section.  $\varphi$  angles and position of the axes are marked on the circumference. The self-rotation function was calculated using a Patterson radius of 35  $\text{\AA}$ , an inner radius cutoff of 5  $\text{\AA}$  and data between 10 and 6  $\text{\AA}$  resolution. All calculations were performed using the program *POLARRFN* in the *CCP4* program package (Collaborative Computational Project, Number 4, 1994). The peaks are scaled from 0 to 100%, 100% representing the origin peak. Contour lines are plotted for all peaks greater than 20% of the origin peak, in intervals of 5%. The unique twofold axis is marked with an arrow.

The authors would like to thank Steve Ealick and colleagues at CHESS for access to these facilities. This work is supported by a grant from the NIH (GM29332) to RTB.

## References

- Abeles, R. H., Fish, S. & Lapinskas, B. (1982). *Biochemistry*, **21**, 5557–5562.
- Bitoni, A. J., Baumann, J., Jarvi, T., McCarthy, J. R. & McCann, P. P. (1990). *Biochem. Pharmacol.* **40**, 601–606.
- Borchardt, R. T. (1980). *J. Med. Chem.* **23**, 357–364.
- Collaborative Computational Project, Number 4 (1994). *Acta Cryst. D50*, 760–763.
- Coulter-Karis, D. E. & Hershfield, M. S. (1989). *Ann. Hum. Genet.* **53**, 169–175.
- Coulter-Karis, D. E. & Hershfield, M. S. (1990). Personal communication.
- Eloranta, T. O. & Kajander, E. O. (1984). *Biochem. J.* **224**, 137–44.
- Eloranta, T. O., Kajander, E. O. & Raina, A. M. (1982). *Med. Biol.* **60**, 272–77.
- Fujioka, M. & Takata, Y. (1981). *J. Biol. Chem.* **256**, 1631–1635.
- de la Haba, G. & Cantoni, G. (1959). *J. Biol. Chem.* **234**, 603–608.
- Henderson, D. M., Hanson, S., Allen, T., Wilson, K., Coulter-Karis, D. E., Greenberg, M. L., Hershfield, M. S. & Ullman, B. (1992). *Mol. Biochem. Parasitol.* **53**, 169–184.
- Hershfield, M. S. (1979). *J. Biol. Chem.* **254**, 22–25.
- Hershfield, M. S., Aiyar, V. M., Premakumar, R. & Small, W. C. (1985). *Biochem. J.* **230**, 43–52.
- Hershfield, M. S. & Kredich, N. M. (1978). *Science*, **202**, 757–760.
- Hershfield, M. S., Kredich, N. M., Ownby, D. R., Ownby, H. & Buckley, R. (1979). *J. Clin. Invest.* **63**, 807–811.
- Hershfield, M. S., Small, W. C., Premakumar, R., Bagnara, A. S. & Fetter, J. E. (1982). In *Biochemistry of S-Adenosylmethionine and Related Compounds*, edited by R. T. Borchardt, E. Usdin & C. R. Creveling, p. 657. London: Macmillan.
- Jancarik, J. & Kim, S.-H. (1991). *J. Appl. Cryst.* **24**, 409–411.
- Kasir, J., Aksamit, R. R., Backlund, P. S. Jr & Cantoni, G. L. (1988). *Biochem. Biophys. Res. Commun.* **153**, 359–364.
- Kredich, N. M. & Martin, D. W. Jr (1977). *Cell*, **12**, 931–938.
- Liu, S., Wolfe, M. S. & Borchardt, R. T. (1992). *Antiviral Res.* **19**, 247–265.
- Matthews, B. W. (1968). *J. Mol. Biol.* **33**, 491–497.
- Migchielsen, A. A., Bruer, M. L., van Roon, M. A., te Riele, H., Zurcher, C., Ossendorp, F., Toutain, S., Hershfield, M. S., Berns, A. & Valerio, D. (1995). *Nature Genet.* **10**, 279–287.
- Miller, M. W., Duhl, D. M., Winkes, B. M., Arredondo-Vega, F., Saxon, P. J., Wolff, G. L., Epstein, C. J., Hershfield, M. S. & Barsh, G. S. (1994). *EMBO J.* **13**, 1806–1816.
- Otwinowski, Z. (1993). *DENZO: An oscillation data processing suite for Macromolecular Crystallography*. Denzo 1.2.1. ed.
- Paisley, S. D., Hasobe, M. & Borchardt, R. T. (1989). *Nucleosides Nucleotides*, **8**, 689–698.
- Palmer, J. L. & Abeles, R. H. (1976). *J. Biol. Chem.* **251**, 5817–5819.
- Palmer, J. L. & Abeles, R. H. (1979). *J. Biol. Chem.* **254**, 1217–1226.
- Richards, H. H., Chiang, P. K. & Cantoni, G. L. (1978). *J. Biol. Chem.* **253**, 4476–4480.
- Ueland, P. M. (1982). *Int. J. Biochem.* **14**, 207–213.
- Wolfe, M. S. & Borchardt, R. T. (1991). *J. Med. Chem.* **34**, 1521–1530.
- Wolos, J. A., Frondorf, K. A., Babcock, G. F., Stripp, S. A. & Bowlin, T. L. (1993). *Cell Immunol.* **149**, 402–408.
- Wolos, J. A., Frondorf, K. A., Davics, G. F., Jarvi, E. T., McCarthy, J. R. & Bowlin, T. L. (1993). *J. Immunol.* **150**, 3264–3273.
- Wolos, J. A., Frondorf, K. A. & Esser, R. E. (1993). *J. Immunol.* **151**, 526–534.
- Yuan, C. S., Yeh, J., Liu, S. & Borchardt, R. T. (1993). *J. Biol. Chem.* **268**, 17030–17037.